

# libGroomRL: Reinforcement Learning for Jets

Stefano Carrazza

*TIF Lab, Dipartimento di Fisica, Università degli Studi di Milano and INFN Milan,  
Via Celoria 16, 20133, Milano, Italy*

Frédéric A. Dreyer

*Rudolf Peierls Centre for Theoretical Physics, University of Oxford,  
Clarendon Laboratory, Parks Road, Oxford OX1 3PU*

In these proceedings, we present a library allowing for straightforward calls in C++ to jet grooming algorithms trained with deep reinforcement learning. The RL agent is trained with a reward function constructed to optimize the groomed jet properties, using both signal and background samples in a simultaneous multi-level training. We show that the grooming algorithm derived from the deep RL agent can match state-of-the-art techniques used at the Large Hadron Collider, resulting in improved mass resolution for boosted objects. Given a suitable reward function, the agent learns how to train a policy which optimally removes soft wide-angle radiation, allowing for a modular grooming technique that can be applied in a wide range of contexts. The neural network trained with `GroomRL` can be used in a `FastJet` analysis through the `libGroomRL` C++ library.

## I. INTRODUCTION

Jets are one of the most common objects appearing in proton-proton colliders such as the Large Hadron Collider (LHC) at CERN. They are defined as collimated bunches of high-energy particles, which emerge from the interactions of quarks and gluons, the fundamental constituents of the proton. In modern analyses, final-state particle momenta (i.e. the product of mass and velocity of the outgoing particles) are mapped to jet momenta using a sequential recombination algorithm with a single free parameter, the jet radius  $R$ , which defines up to which angle particles can get recombined into a given jet [3].

Due to the very high energies of its collisions, the LHC is routinely producing heavy particles with transverse momenta, the momentum component transverse to the beam axis, far greater than their rest mass. When these objects are sufficiently energetic (or boosted), they can often generate very collimated decays, which are then reconstructed as a single fat jet, whose radiation patterns differ from standard quark or gluon jets. Since the advent of the LHC program, the study of the substructure of jets has matured into a remarkably active field of research that has become notably conducive to applications of recent Machine Learning techniques [8, 9, 14].

A particularly useful set of tools for experimental analyses are jet grooming algorithms, defined as a post-processing treatment of jets to remove unenergetic wide-angle radiation which is not associated with the underlying hard substructure. Grooming techniques play a crucial role in Standard Model measurements [1, 17] and in improving the boson- and top-tagging efficiencies at the LHC.

In these proceedings, we describe the `GroomRL` framework [4], which is used to train a grooming algorithm using reinforcement learning (RL), and introduce the `libGroomRL` C++ library which makes it straightforward to use the resulting grooming strategy in a real analysis.

To train the RL agent, we decompose the problem of jet grooming into successive steps for which a reward function can be designed taking into account the physical features that characterize such a system. We then use a modified implementation of a Deep Q-Network (DQN) agent [15, 16] and train a dense neural network (NN) to optimally remove radiation unassociated from the core of the jet. The trained model can then be applied on other data sets, showing improved resolution compared to state-of-the-art techniques as well as a strong resilience to non-perturbative effects. The framework and data used in this paper are available as open-source and published material in [5–7].<sup>1</sup>

## II. JET REPRESENTATION

Let us start by introducing the representation we use for jets. We take the particle constituents of a jet, as defined by any modern algorithm, and recombine them using a Cambridge/Aachen (CA) sequential clustering algorithm [10]. The CA algorithm does a pairwise recombination, adding together the momenta of the two particles with the closest distance as defined by the measure

$$\Delta_{ij}^2 = (y_i - y_j)^2 + (\phi_i - \phi_j)^2, \quad (1)$$

where  $y_i$  is the rapidity, a measure of relativistic velocity along the beam axis, and  $\phi_i$  is the azimuthal angle of particle  $i$  around the same axis. This clustering sequence is then used to recast the jet as a full binary tree, where each of the nodes contains information about the kinematic properties of the two parent particles. For each

---

<sup>1</sup> The code is available at <https://github.com/JetsGame/GroomRL>, along with a C++ library at <https://github.com/JetsGame/libGroomRL>.

node  $i$  of the tree we define an object  $\mathcal{T}^{(i)}$  containing the current observable state  $s_t$ , as well as a pointer to the two children nodes and one to the parent node. The children nodes  $a$  and  $b$  are ordered in transverse momentum such that  $p_{t,a} > p_{t,b}$ , and we label  $a$  the “harder” child and  $b$  the “softer” one. The set of possible states is defined by a five dimensional box, such that the state of the node is a tuple

$$s_t = \{z, \Delta_{ab}, \psi, m, k_t\}, \quad (2)$$

where  $z = p_{t,b}/(p_{t,a} + p_{t,b})$  is the momentum fraction of the softer child  $b$ ,  $\psi = \tan^{-1}(\frac{y_b - y_a}{\phi_a - \phi_b})$  is the azimuthal angle around the  $i$  axis,  $m$  is the mass, and  $k_t = p_{t,b}\Delta_{ab}$  is the transverse momentum of  $b$  relative to  $a$ .

### A. Grooming algorithm

A grooming algorithm acting on a jet tree can be defined by a simple recursive procedure which follows each of the branches and uses a policy  $\pi_g(s_t)$  to decide based on the values of the current tuple  $s_t$  whether to remove the softer of the two branches. This is shown in Algorithm 1, where the minus sign is understood to mean the update of the kinematics of a node after removal of a soft branch. The grooming policy  $\pi_g(s_t)$  returns an action  $a_t \in \{0, 1\}$ , with  $a_t = 1$  corresponding to the removal of a branch, and  $a_t = 0$  leaving the node unchanged. The state  $s_t$  is used to evaluate the current action-values  $Q^*(s, a)$  for each possible action, which in turn are used to determine the best action at this step through a greedy policy.

It is easy to translate modern grooming algorithms in this language. For example, Recursive Soft Drop (RSD) [11] corresponds to a policy

$$\pi_{\text{RSD}}(s_t) = \begin{cases} 0 & \text{if } z > z_{\text{cut}} \left(\frac{\Delta_{ab}}{R_0}\right)^\beta, \\ 1 & \text{else,} \end{cases} \quad (3)$$

where  $z_{\text{cut}}$ ,  $\beta$  and  $R_0$  are the parameters of the algorithm, and 1 corresponds as before to the action of removing the tree branch with smaller transverse momentum.

## III. SETTING UP A GROOMING ENVIRONMENT

In order to find an optimal grooming policy  $\pi_g$ , we introduce an environment and a reward function, formulating the problem in a way that can be solved using a RL algorithm.

We initialize a list of all trees used for the training, from which a tree is randomly selected at the beginning of each episode. Each step consists in taking the node with the largest  $\Delta_{ab}$  value and taking an action on which of its branches to keep based on the state  $s_t$  of that node. Once a decision has been taken on the removal of the

---

### Algorithm 1 Grooming

---

**Input:** policy  $\pi_g$ , binary tree node  $\mathcal{T}^{(i)}$   
 $a_t = \pi_g(\mathcal{T}^{(i)} \rightarrow s_t)$   
**if**  $a_t == 1$  **then**  
     $\mathcal{T}^{(j)} = \mathcal{T}^{(i)}$   
    **while**  $\mathcal{T}^{(j)} = (\mathcal{T}^{(j)} \rightarrow \text{parent})$  **do**  
         $\mathcal{T}^{(j)} \rightarrow s_t = (\mathcal{T}^{(j)} \rightarrow s_t) - (\mathcal{T}^{(i)} \rightarrow b \rightarrow s_t)$   
    **end while**  
     $\mathcal{T}^{(i)} = (\mathcal{T}^{(i)} \rightarrow a)$   
    Grooming( $\pi_g, \mathcal{T}^{(i)}$ )  
**else**  
    Grooming( $\pi_g, \mathcal{T}^{(i)} \rightarrow a$ )  
    Grooming( $\pi_g, \mathcal{T}^{(i)} \rightarrow b$ )  
**end if**

---

softer branch, and the parent nodes have been updated accordingly, the remaining children of the node are added to the list of nodes to consider in a following step of this episode. The reward function is then evaluated using the current state of the tree. The episode terminates once all nodes have been iterated over.

The framework described here deviates from usual RL implementations in that the range of possible states for any episode are fixed at the start. The transition probability between states  $\mathcal{P}(s_{t+1}|s_t, a_t)$  therefore does not always depend very strongly on the action, although a grooming action can result in the removal of some of the future states and will therefore still have an effect on the distribution.

### A. Finding optimal hyper-parameters

The optimal choice of hyper-parameters, both for the model architecture and for the grooming parameters, is determined using the distributed asynchronous hyper-parameter optimization library `hyperopt` [2].

The performance of an agent is evaluated by defining a loss function, which is evaluated on a distinct validation set consisting of 50k signal and background jets. For each sample, we evaluate the jet mass after grooming of each jet and derive the corresponding distribution. To calculate the loss function  $\mathcal{L}$ , we start by determining a window  $(w_{\text{min}}, w_{\text{max}})$  containing a fraction  $f = 0.6$  of the final jet masses of the groomed signal distribution, defining  $w_{\text{med}}$  as the median value on that interval. The loss function is then defined as

$$\mathcal{L} = \frac{1}{5} |w_{\text{max}} - w_{\text{min}}| + |m_{\text{target}} - w_{\text{med}}| + 20f_{\text{bkg}}, \quad (4)$$

where  $f_{\text{bkg}}$  is the fraction of the groomed background sample contained in the same interval, and  $m_{\text{target}}$  is a reference value for the signal.

We scan hyper-parameters using 1000 iterations and select the ones for which the loss  $\mathcal{L}$  evaluated on the validation set is minimal. In practice we will do three different scans: to determine the best parameters of the reward function, to find an optimal grooming environment,

and to determine the architecture of the DQN agent. The scan is performed by requiring `hyperopt` to use a uniform search space for continuous parameters, a log-uniform search space for the learning rate and a binary choice for all integer or boolean parameters. The optimization used in all the results presented in this work rely on the Tree-structured Parzen Estimator (TPE) algorithm.

## B. Defining a reward function

One of the key ingredients for the optimization of the grooming policy is the reward function used at each step during the training. We consider a reward with two components: a first piece evaluated on the full tree, and another that considers only the kinematics of the current node.

The first component of the reward compares the mass of the current jet to a set target mass, typically the mass of the underlying boosted object. We implement this mass reward using a Cauchy distribution, which has two free parameters, the target mass  $m_{\text{target}}$  and a width  $\Gamma$ , so that

$$R_M(m) = \frac{\Gamma^2}{\pi(|m - m_{\text{target}}|^2 + \Gamma^2)}. \quad (5)$$

Separately, we calculate a reward on the current node which gives a positive reward for the removal of wide-angle soft radiation, as well as for leaving intact hard-collinear emissions. This provides a baseline behavior for the groomer. We label this reward component ‘‘Soft-Drop’’ due to its similarity with the Soft Drop condition [13], and implement it through exponential distributions

$$R_{\text{SD}}(a_t, \Delta, z) = a_t \min(1, e^{-\alpha_1 \ln(1/\Delta) + \beta_1 \ln(z_1/z)}) + (1 - a_t) \max(0, 1 - e^{-\alpha_2 \ln(1/\Delta) + \beta_2 \ln(z_2/z)}), \quad (6)$$

where  $a_t = 0, 1$  is the action taken by the policy, and  $\alpha_i, \beta_i, z_i$  are free parameters.

The total reward function is then given by

$$R(m, a_t, \Delta, z) = R_M(m) + \frac{1}{N_{\text{SD}}} R_{\text{SD}}(a_t, \Delta, z). \quad (7)$$

Here  $N_{\text{SD}}$  is a normalization factor determining the weight given to the second component of the reward.

## C. RL implementation and multi-level training

For the applications in this paper, we have implemented a DQN agent that contains a groomer module, which is defined by the underlying NN model and the test policy used by the agent. The groomer can be extracted after the model has been trained, using a greedy policy to select the best action based on the  $Q$ -values predicted

by the NN. This allows for straightforward application of the resulting grooming strategy on new samples.

The training sample consists of 500k signal and background jets simulated using `Pythia 8.223` [18]. We will construct two separate models by considering two signal samples, one with boosted  $W$  jets and one with boosted top jets, while the background always consists of QCD jets. We use the  $WW$  and  $t\bar{t}$  processes, with hadronically decaying  $W$  and top, to create the signal samples, and the dijet process for the background. All samples used in this article can be available online [6]. The grooming environment is initialized by reading in the training data and creating an event array containing the corresponding jet trees.

To train the RL agent, we use a multi-level approach taking into account both signal and background samples. At the beginning of each episode, we select either a signal jet or a background jet, with probability  $1 - p_{\text{bkg}}$ . For signal jets, the reward function uses a reference mass set to the  $W$ -boson mass,  $m_{\text{target}} = m_W$ , or to the top mass,  $m_{\text{target}} = m_t$ , depending on the choice of sample. In the case of the background the mass reward function in equation (7) is changed to

$$R_M^{\text{bkg}}(m) = \frac{m}{\Gamma_{\text{bkg}}} \exp\left(-\frac{m}{\Gamma_{\text{bkg}}}\right). \quad (8)$$

The width parameters  $\Gamma, \Gamma_{\text{bkg}}$  are also set to different values for signal and background reward functions, and are determined through a hyper-parameter scan.

We found that while this multi-level training only marginally improves the performance, it noticeably reduces the variability of the model.

## IV. JET MASS SPECTRUM

Let us now apply the `GroomRL` models to new data samples. We consider three test sets of 50k elements each: one with QCD jets, one with  $W$  initiated jets and one with top jets. The size of the window containing 60% of the mass spectrum of the  $W$  sample, as well as the corresponding median value, are given in table I for each different grooming strategy. As a benchmark, we compare to the RSD algorithm, using parameters  $z_{\text{cut}} = 0.05, \beta = 1$  and  $R_0 = 1$ . One can notice a sizeable reduction of the window size after grooming with the machine learning based algorithms, while all groomers are able to reconstruct the peak location to a value very close to the  $W$  mass.

The distribution of the jet mass after grooming for each of these samples is shown in figure 1. Each curve gives the differential cross section  $d\sigma/dm_j$  normalized by the total cross section. We show results for the grooming algorithm trained on a  $W$  sample, as well as for the ungroomed (or plain) jet mass and the jet mass after RSD grooming. As expected, one can observe that for the ungroomed case the resolution is very poor, with the

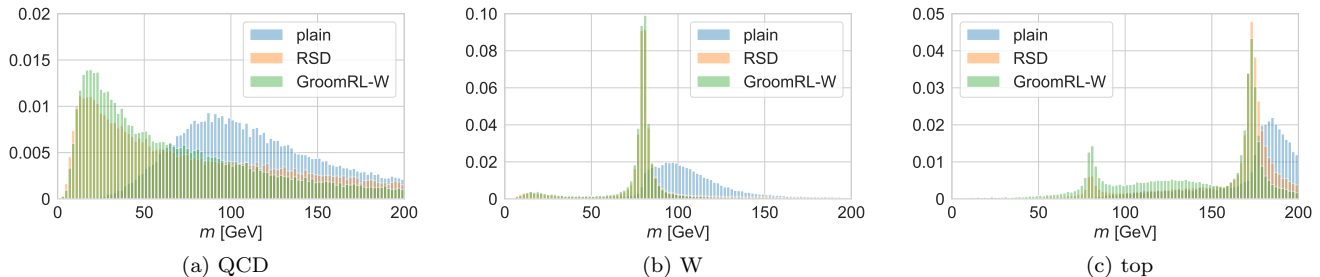


FIG. 1: Jet mass spectrum for (a) QCD jets, (b)  $W$  jets, (c) top jets. The **GroomRL-W** curve is obtained from training on  $W$  data.

TABLE I: Size of the window  $\Delta w$  containing 60% of the  $W$  mass spectrum, and median value on that interval.

	PLAIN	GRL-W	GRL-Top	RSD
$\Delta w$ [GeV]	44.65	10.70	13.88	16.96
$w_{\text{med}}$ [GeV]	104.64	80.09	80.46	80.46

QCD jets having large masses due to wide-angle radiation, while the  $W$  and top mass peaks are heavily distorted. In contrast, after applying RSD or **GroomRL**, the jet mass is reconstructed much more accurately. One interesting feature of **GroomRL** is that it is able to lower the jet mass for quark and gluon jets, further reducing the background contamination in windows close to a heavy particle mass.

In top jets, displayed in figure 1c, there are also noticeable enhancements after grooming with **GroomRL**, despite the fact that the training did not involve any top-related data. This demonstrates that the tools derived from our framework are robust and can be applied to data sets beyond their training range with good results.

## V. CONCLUSIONS

We have shown a promising application of RL to the issue of jet grooming. Using a carefully designed reward function, we have constructed a groomer from a dense NN trained with a DQN agent.

This grooming algorithm was then applied to a range of data samples, showing excellent results for the mass resolution of boosted heavy particles. In particular, while the training of the NN is performed on samples consisting of  $W$  (or top) jets, the groomer yields noticeable gains in the top (or  $W$ ) case as well, on data outside of the training range.

The improvements in resolution and background reduction compared to alternative state-of-the-art methods provide an encouraging demonstration of the relevance of machine learning for jet grooming. In particular, we showed that it is possible for a RL agent to extract the

underlying physics of jet grooming and distill this knowledge into an efficient algorithm.

Due to its simplicity, the model we developed also retains most of the calculability of other existing methods such as Soft Drop. Accurate numerical computations of groomed jet observables are therefore achievable, allowing for the possibility of direct comparisons with data. Furthermore, given an appropriate sample, one could also attempt to train the grooming strategy on real data, bypassing some of the limitations due to the use of parton shower programs.

The **GroomRL** framework, available online [5], is generic and can easily be extended to higher-dimensional inputs, for example to consider multiple emissions per step or additional kinematic information. Algorithms derived from **GroomRL** can easily be used to analyze real events through the associated `libGroomRL` C++ library [7]. While the method presented in this article was applied to a specific problem in particle physics, we expect that with a suitable choice of reward function, this framework is in principle also applicable to a range of problems where a tree requires pruning.

**Acknowledgments:** We are grateful to Jia-Jie Zhu and Gavin Salam for comments on the manuscript and to Jesse Thaler for useful discussions. We also acknowledge the NVIDIA Corporation for the donation of a Titan Xp GPU used for this research. F.D. is supported by the Science and Technology Facilities Council (STFC) under grant ST/P000770/1. S.C. is supported by the European Research Council under the European Union’s Horizon 2020 research and innovation Programme (grant agreement number 740006).

## Appendix A: Determining the RL agent

The DQN agent uses an Adam optimizer [12], and the training is performed with a Boltzmann policy, which chooses an action according to weighted probabilities, with the current best action being the likeliest.

Let us now determine the remaining parameters of the DQN agent. To this end, we perform two independent scans, for the grooming environment and for the network

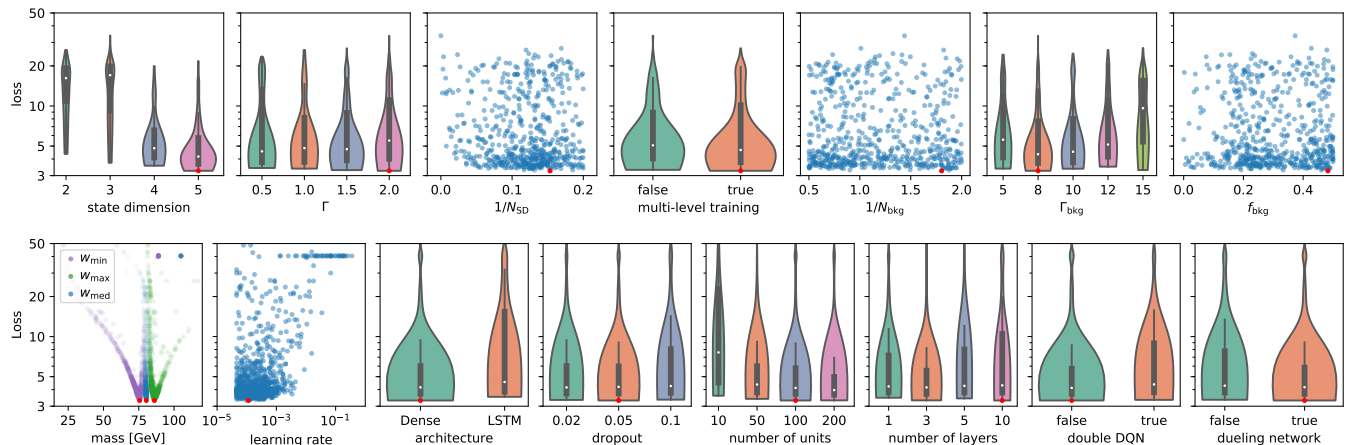


FIG. 2: Distribution of the loss value for different parameters. The best performing model is indicated in red.

architecture.

The grooming environment has several options, which are shown in the upper row of figure 2. Here the distribution of loss values for discrete options are displayed using violin plots, showing both the probability density of the loss values as well as its quartiles. The first plot is the dimensionality of the state observed at each step, which can be a subset of the tuple given in equation (2). We can observe that as the dimension of the input state is increased, the NN is able to leverage this additional information, leading to a decrease of the loss function. The scan over the normalization parameters of the reward functions shows that it is preferable to use a small width  $\Gamma$  for the signal, with a large value  $\Gamma_{\text{bkg}}$  for the background, as well as a small value for the  $1/N_{\text{SD}}$  factor. One can also see that the multi-level training described in section III C leads to a distribution of loss values concentrated at smaller values. We have also allowed for several functional forms of the signal mass reward function, although for our final model we will use a Cauchy distribution.

The parameters of the network architecture are shown in the lower row of figure 2, with the first plot showing the mass window containing 60% of the signal distribution, with the median of that interval shown in blue. The scatter plot of the learning rate used for the Adam optimizer shows that a value slightly above  $10^{-4}$  yields the best result. The scan shows a preference for a dense network with a large number of units and layers as well as a dropout layer as the architecture of the NN. Finally, we see that using duelling networks [20] leads to a small improvement of the model, while double Q-learning [19] does not.

## Appendix B: Optimal GroomRL model

The final GroomRL model is trained using the full training sample with 500k signal/background jets for 1M

TABLE II: Final parameters for GroomRL, with the two values of  $m_{\text{target}}$  corresponding to the  $W$  and top mass.

Parameters	Value
$m_{\text{target}}$	80.385 GeV OR 173.2 GeV
$s_t$ DIMENSION	5
$\Gamma$	2 GeV
$(\alpha_1, \beta_1, \ln z_1)$	(0.59, 0.18, -0.92)
$(\alpha_2, \beta_2, \ln z_2)$	(0.65, 0.33, -3.53)
$1/N_{\text{SD}}$	0.15
MULTI-LEVEL TRAINING	YES
$\Gamma_{\text{bkg}}$	8 GeV
$1/N_{\text{bkg}}$	1.8 OR 1.0
$p_{\text{bkg}}$	0.48 OR 0.2
LEARNING RATE	$10^{-4}$
DUELING NN	YES
DOUBLE DQN	NO
$N_{\text{epochs}}^{\text{max}}$	500K
ARCHITECTURE	DENSE
DROPOUT	0.05
LAYERS	10
NODES	100

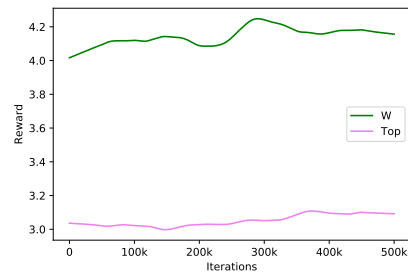


FIG. 3: Reward evolution during training of the GroomRL on  $W$  and top data. A LOESS smoothing is applied to the original curves.

epochs. The overall training time requires four hours of training using a single NVIDIA GTX 1080 Ti GPU with 12 GB of memory which includes all the training jet trees and the DQN parameters.

The parameters of the best GroomRL model obtained following the strategy presented in this paper is listed in table II. Here two values are given for the  $m_{\text{target}}$  parameter, which are used to train on either a sample consisting

of  $W$  bosons or of top quarks.

In figure 3 we show the reward value during the training of the GroomRL for  $W$  bosons and top quarks, after applying the LOESS smoothing algorithm on the original curve. We observe an improvement of the reward function during the first 300k training epochs, with the reward becoming relatively stable after that point.

- 
- [1] Aaboud, M. et al. Measurement of the Soft-Drop Jet Mass in pp Collisions at  $\sqrt{s} = 13$  TeV with the ATLAS Detector. *Phys. Rev. Lett.*, 121(9):092001, 2018. doi: 10.1103/PhysRevLett.121.092001.
- [2] Bergstra, J., Yamins, D., and Cox, D. D. Making a science of model search: Hyperparameter optimization in hundreds of dimensions for vision architectures. In *Proceedings of the 30th International Conference on International Conference on Machine Learning - Volume 28*, ICML'13, pp. I–115–I–123. JMLR.org, 2013.
- [3] Cacciari, M., Salam, G. P., and Soyez, G. The anti- $k_t$  jet clustering algorithm. *JHEP*, 04:063, 2008. doi: 10.1088/1126-6708/2008/04/063.
- [4] Carrazza, S. and Dreyer, F. A. Jet grooming through reinforcement learning. 2019.
- [5] Carrazza, S. and Dreyer, F. A. JetsGame/GroomRL v1.0.0, March 2019. URL <https://doi.org/10.5281/zenodo.2602529>.
- [6] Carrazza, S. and Dreyer, F. A. JetsGame/data v1.0.0, March 2019. URL <https://doi.org/10.5281/zenodo.2602514>. This repository is git-lfs.
- [7] Carrazza, S. and Dreyer, F. A. JetsGame/libGroomRL v1.0.0, July 2019. URL <https://doi.org/10.5281/zenodo.3265835>.
- [8] Datta, K. and Larkoski, A. How Much Information is in a Jet? *JHEP*, 06:073, 2017. doi: 10.1007/JHEP06(2017)073.
- [9] de Oliveira, L., Kagan, M., Mackey, L., Nachman, B., and Schwartzman, A. Jet-images deep learning edition. *JHEP*, 07:069, 2016. doi: 10.1007/JHEP07(2016)069.
- [10] Dokshitzer, Y. L., Leder, G. D., Moretti, S., and Webber, B. R. Better jet clustering algorithms. *JHEP*, 08:001, 1997. doi: 10.1088/1126-6708/1997/08/001.
- [11] Dreyer, F. A., Necib, L., Soyez, G., and Thaler, J. Recursive Soft Drop. *JHEP*, 06:093, 2018. doi: 10.1007/JHEP06(2018)093.
- [12] Kingma, D. P. and Ba, J. Adam: A method for stochastic optimization. *CoRR*, abs/1412.6980, 2014. URL <http://arxiv.org/abs/1412.6980>.
- [13] Larkoski, A. J., Marzani, S., Soyez, G., and Thaler, J. Soft Drop. *JHEP*, 05:146, 2014. doi: 10.1007/JHEP05(2014)146.
- [14] Louppe, G., Cho, K., Becot, C., and Cranmer, K. QCD-Aware Recursive Neural Networks for Jet Physics. *JHEP*, 01:057, 2019. doi: 10.1007/JHEP01(2019)057.
- [15] Mnih, V., Kavukcuoglu, K., Silver, D., Graves, A., Antonoglou, I., Wierstra, D., and Riedmiller, M. A. Playing atari with deep reinforcement learning. *CoRR*, abs/1312.5602, 2013. URL <http://arxiv.org/abs/1312.5602>.
- [16] Mnih, V., Kavukcuoglu, K., Silver, D., Rusu, A. A., Veness, J., Bellemare, M. G., Graves, A., Riedmiller, M., Fidjeland, A. K., Ostrovski, G., Petersen, S., Beattie, C., Sadik, A., Antonoglou, I., King, H., Kumaran, D., Wierstra, D., Legg, S., and Hassabis, D. Human-level control through deep reinforcement learning. *Nature*, 518(7540):529–533, February 2015. ISSN 00280836. URL <http://dx.doi.org/10.1038/nature14236>.
- [17] Sirunyan, A. M. et al. Measurements of the differential jet cross section as a function of the jet mass in dijet events from proton-proton collisions at  $\sqrt{s} = 13$  TeV. *JHEP*, 11:113, 2018. doi: 10.1007/JHEP11(2018)113.
- [18] Sjöstrand, T., Ask, S., Christiansen, J. R., Corke, R., Desai, N., Ilten, P., Mrenna, S., Prestel, S., Rasmussen, C. O., and Skands, P. Z. An Introduction to PYTHIA 8.2. *Comput. Phys. Commun.*, 191:159–177, 2015. doi: 10.1016/j.cpc.2015.01.024.
- [19] van Hasselt, H., Guez, A., and Silver, D. Deep reinforcement learning with double q-learning. *CoRR*, abs/1509.06461, 2015. URL <http://arxiv.org/abs/1509.06461>.
- [20] Wang, Z., de Freitas, N., and Lanctot, M. Dueling network architectures for deep reinforcement learning. *CoRR*, abs/1511.06581, 2015. URL <http://arxiv.org/abs/1511.06581>.